

Synthesis, Crystal Structure, and Magnetic and Electronic Properties of the Caesium-based Transition Metal Halide Cs₃Fe₂Br₉

Fengxia Wei,^{a,b} Federico Brivio,^a Yue Wu,^a Shijing Sun,^a Paul D. Bristowe^{a*} and Anthony K. Cheetham^{a*}

^aDepartment of Materials Science and Metallurgy, University of Cambridge, CB3 0FS, UK

^bInstitute of Materials Research and Engineering, Agency for Science, Technology and Research, 2 Fusionopolis Way, Singapore.

Table of contents

Details of methods including single crystal X-ray diffraction, DFT calculations, and magnetic susceptibility fitting formula.

Figure S1. Crystal structure of Cs₂NaFeCl₆: purple - FeCl₆ octahedra, brown - NaCl₆ octahedra; Cs is in the cavity of 3D octahedral framework. Space group: *Fm* $\bar{3}$ *m*, cubic, a = 10.3403(1) Å. Crystal colour: red. CCDC No. 1575067.

Figure S2. Structure of Cs₂FeBr₅·H₂O: the distorted FeBr₅O is shown in brown, oxygen is red with H attached. a = 14.6652(3) Å, b = 10.4144(2) Å and c = 7.5110(2) Å, space group *Pnma*. CCDC No. 1575069.

Figure S3. Crystal structure of CsFeBr₄: Purple - FeBr₄ tetrahedra. Space group: *Pnma*, orthorhombic, a = 12.0861(5) Å, b = 7.4271(3) Å, c = 9.8187(4) Å. Crystal colour: brown. CCDC No. 1575070.

Figure S4. Interatomic distances and octahedral angles - variations as a function of temperature.

Figure S5. Thermogravimetric analysis curve for Cs₃Bi₂I₉.

Figure S6. Thermogravimetric analysis curve for MA₃Bi₂I₉.

Figure S7. Curie-Weiss fitting for the paramagnetic region of Cs₃Fe₂Br₉, (a) for χ and (b) for 1/ χ to obtain the Weiss constant (fitted from 50 K to 300 K).

Table S1. DFT calculated atomic structure (fractional coordinates) of Cs₃Fe₂Br₉.

Table S2. DFT calculated energy differences between different magnetically ordered states of Cs₃Fe₂Br₉ relative to the most stable configuration (i.e. AFM-3). U: spin up, D: spin down.

Details of methods

Experimental

Crystal structure determination was carried out using an Oxford Gemini E Ultra diffractometer, Mo K α radiation ($\lambda = 0.71073 \text{ \AA}$), equipped with an Eos CCD detector. Variable temperature data were collected from 300 K to 120 K using a Cryo system under liquid nitrogen flow with 30 K steps; the crystal stayed under nitrogen flow for 10 mins at each temperature, allowing sufficient time for cooling. Data collection and reduction were conducted using CrysAliPro. An empirical absorption correction was applied with the Olex2 platform, and the structure was solved using ShelXS¹ and refined with ShelXL.²

Computational

A plane-wave cut-off of 600 eV and a 6x6x1 k-point grid centred on the Γ point was used during geometry optimisation of Cs₃Fe₂Br₉. For the band structure calculation using HSE06 the plane wave cut-off was reduced to 500 eV. The optimised atomic structure is given in Table S1.

Three possible anti-ferromagnetic (AFM) configurations labelled UU-DD (AFM-1), UD-DU (AFM-2) and UD-UD (AFM-3) were considered for the four Fe atoms in a unit cell, where U denotes spin up and D denotes spin down. The energies of these configurations are compared to the ferromagnetic (FM) and non-magnetic (NM) cases in Table S2. The most stable configuration is the one where next neighbour Fe atoms have opposite spin orientation.

Formula for fitting magnetic susceptibility

The magnetic susceptibility can be expressed by intradimer J and interdimer interactions J_p + J_c:

$$\chi(T) = \chi_o(T) / [1 - 3(J_p + J_c) \cdot \frac{\chi_o(T)}{(g^2 \mu_B^2 N_A)}]$$

and

$$\chi_o(T) = \left[\frac{2N_A g^2 \mu_B^2}{kTZ} \right] \left[\exp\left(\frac{J}{kT}\right) + 5\exp\left(\frac{3J}{kT}\right) + 14\exp\left(\frac{6J}{kT}\right) \right]$$

with

$$Z = 1 + 3\exp\left(\frac{J}{kT}\right) + 5\exp\left(\frac{3J}{kT}\right) + 7\exp\left(\frac{6J}{kT}\right)$$

where N_A is Avogadro's number, μ_B is the Bohr magneton, g is a dimensionless magnetic moment or g-value, and k is the Boltzmann constant.

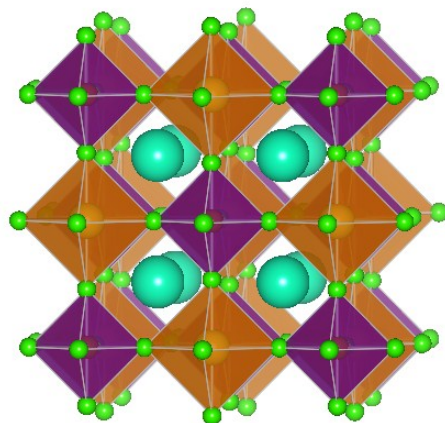


Figure S1. Crystal structure of $\text{Cs}_2\text{NaFeCl}_6$: purple - FeCl_6 octahedra, brown - NaCl_6 octahedra; Cs is in the cavity of 3D octahedral framework. Space group: $Fm\bar{3}m$, cubic, $a = 10.3403(1) \text{ \AA}$. Crystal colour: red. CCDC No. 1575067.

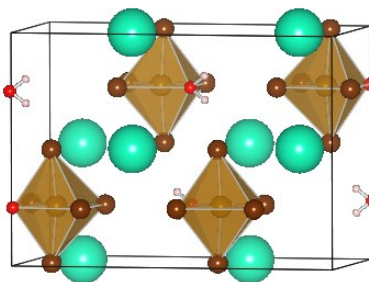


Figure S2. Structure of $\text{Cs}_2\text{FeBr}_5 \cdot \text{H}_2\text{O}$: the distorted FeBr_5O is shown in brown, oxygen is red with H attached. $a = 14.6652(3) \text{ \AA}$, $b = 10.4144(2) \text{ \AA}$ and $c = 7.5110(2) \text{ \AA}$, space group $Pnma$. CCDC No. 1575069.

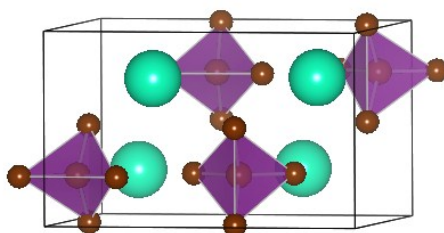


Figure S3. Crystal structure of CsFeBr_4 : Purple - FeBr_4 tetrahedra. Space group: $Pnma$, orthorhombic, $a = 12.0861(5) \text{ \AA}$, $b = 7.4271(3) \text{ \AA}$, $c = 9.8187(4) \text{ \AA}$. Crystal colour: brown. CCDC No. 1575070.

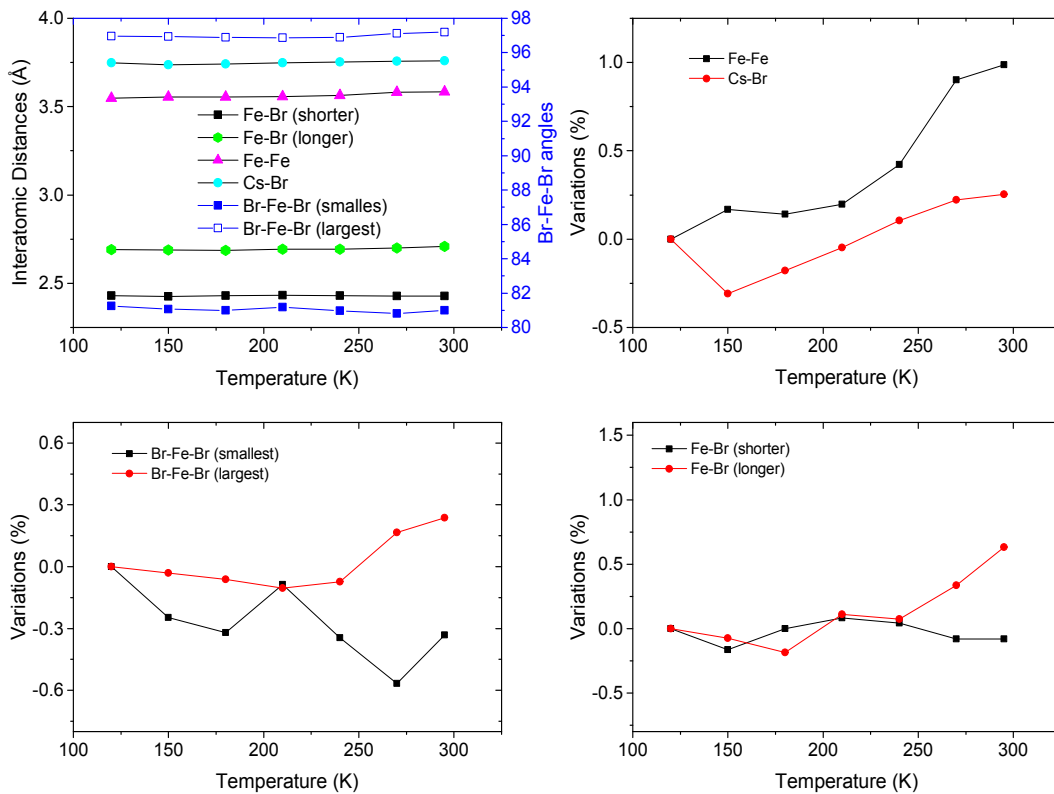


Figure S4. Interatomic distances and octahedral angles - variations as a function of temperature.

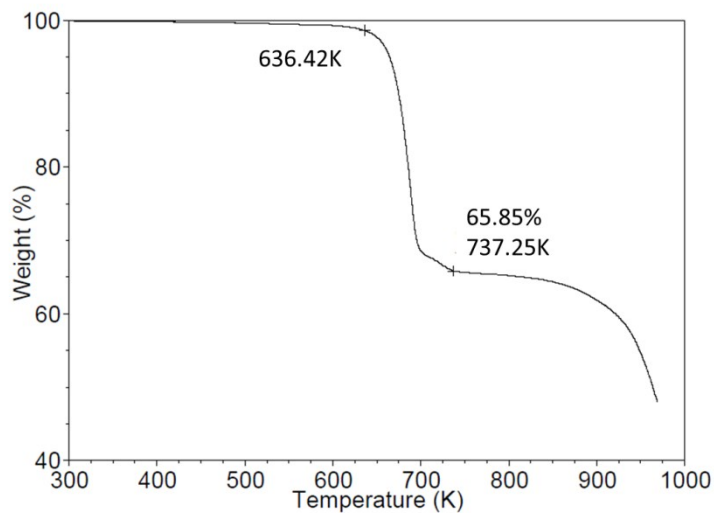


Figure S5. Thermogravimetric analysis curve for $\text{Cs}_3\text{Bi}_2\text{I}_9$.

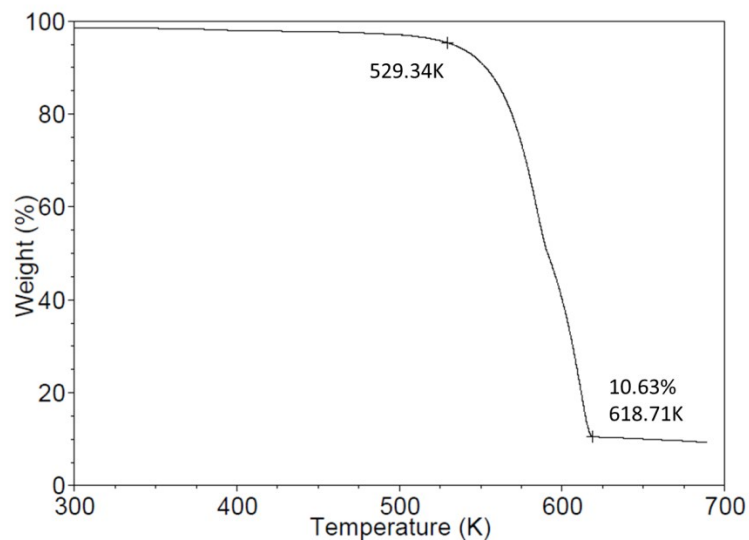


Figure S6. Thermogravimetric analysis curve for $\text{MA}_3\text{Bi}_2\text{I}_9$.

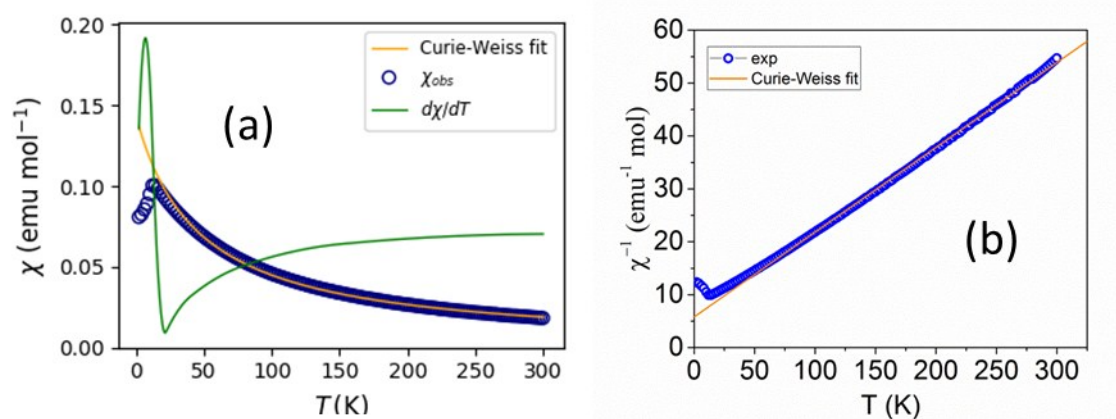


Figure S7. Curie-Weiss fitting for the paramagnetic region of $\text{Cs}_3\text{Fe}_2\text{Br}_9$, (a) for χ and (b) for $1/\chi$ to get the Weiss constant (fitted from 50 K to 300 K).

Table S1. DFT calculated atomic positions of Cs₃Fe₂Br₉. Lattice parameters: a = b = 7.4201 Å, c = 18.3609 Å, α = β = 90°, γ = 120°, vol = 875.467 Å³, density = 4.6642 g/cm³.

No.	label	Fractional coordinates			Orthogonal Coordinates		
		x	y	z	x _o [Å]	y _o [Å]	z _o [Å]
1	Br1	0.036950	0.518475	0.75	-0.2374	3.71	-13.7707
2	Br2	0.963050	0.481525	0.25	-6.1885	0.0000	-4.5902
3	Br3	0.481525	0.518476	0.75	-3.0943	2.0607	-13.7707
4	Br4	0.518475	0.481524	0.25	-3.3317	1.6494	-4.5902
5	Br5	0.481524	0.963050	0.75	-3.0943	5.3594	-13.7707
6	Br6	0.518476	0.036950	0.25	-3.3317	-1.6494	-4.5902
7	Br7	0.180243	0.360485	0.595179	-1.1582	2.0061	-10.928
8	Br8	0.819757	0.639515	0.404821	-5.2677	1.7039	-7.4329
9	Br9	0.639515	0.819758	0.595179	-4.1095	3.71	-10.928
10	Br10	0.360485	0.180242	0.404821	-2.3165	-0.0000	-7.4329
11	Br11	0.180242	0.819757	0.595179	-1.1582	5.4139	-10.928
12	Br12	0.819758	0.180243	0.404821	-5.2677	-1.7039	-7.4329
13	Br13	0.819757	0.639515	0.095179	-5.2677	1.7039	-1.7476
14	Br14	0.180243	0.360485	0.904821	-1.1582	2.0061	-16.6133
15	Br15	0.360485	0.180242	0.095179	-2.3165	-0.0000	-1.7476
16	Br16	0.639515	0.819758	0.904821	-4.1095	3.71	-16.6133
17	Br17	0.819758	0.180243	0.095179	-5.2677	-1.7039	-1.7476
18	Br18	0.180242	0.819757	0.904821	-1.1582	5.4139	-16.6133
19	Cs1	0.000000	0.000000	0.75	0.0000	0	-13.7707
20	Cs2	0.000000	0.000000	0.25	0.0000	0.0000	-4.5902
21	Cs3	0.666667	0.333333	0.571456	-4.2840	0	-10.4925
22	Cs4	0.333333	0.666667	0.428544	-2.1420	3.7100	-7.8685
23	Cs5	0.333333	0.666667	0.071456	-2.1420	3.7100	-1.312
24	Cs6	0.666667	0.333333	0.928544	-4.2840	0	-17.0489
25	Fe1	0.333333	0.666667	0.668257	-2.1420	3.71	-12.2698
26	Fe2	0.666667	0.333333	0.331743	-4.2840	-0.0000	-6.0911
27	Fe3	0.666667	0.333333	0.168257	-4.2840	-0.0000	-3.0894
28	Fe4	0.333333	0.666667	0.831743	-2.1420	3.71	-15.271

Table S2. DFT calculated energy differences between different magnetically ordered states of $\text{Cs}_3\text{Fe}_2\text{Br}_9$ relative to the most stable configuration (i.e. AFM-3). U: spin up, D: spin down.

Configuration	Energy (eV / unit cell)	Energy difference (meV / unit cell)	Energy difference (meV/f.u.)
NM	-101.94543	671	335.5
FM	-102.4561	160	80
AFM-1(UU-DD)	-102.60318	13	6.5
AFM-2 (UD-DU)	-102.45387	162	81
AFM-3 (UD-UD)	-102.6164	0	0

- 1 G. . Sheldrick, *A short Hist. SHELX*, 2008, **64**, 112–122.
- 2 G. M. Sheldrick, *Acta Crystallogr. Sect. C Struct. Chem.*, 2015, **71**, 3–8.